

A DIFFUSION APPROACH FOR ORIENTED VOLUME DATA DENOISING

Romulus TEREDES

Technical University of Cluj-Napoca, Communications Department

26-28 Barițiu Street, Cluj-Napoca, Romania, +40-264-401564, +40-264-401575, Romulus.Terebes@com.utcluj.ro

Abstract: This paper proposes a new method for denoising non-time dependent volumetric oriented data blocks. The method is developed under the partial differential equations theoretical framework and it is defined on orthogonal section planes of the three-dimensional space. The efficiency of the method in denoising oriented volume data is proven using an extensive experimental part involving several random computer-generated synthetic data blocks and statistical interpretations. In the experimental section we also provide a result obtained on real data.

Keywords: diffusion equations, partial differential equations, image restoration

I. INTRODUCTION

Partial differential equations (PDE) - based filters are modeling an image denoising process through a partial differential equation that regards the noisy image $I(x,y)$ as the initial state of a forward diffusion process and relates the image spatial derivatives with a time derivative. A classical method that devoted a lot of interest is the anisotropic diffusion equation which is essentially driven by a non-linear diffusivity function $g(\bullet)$ taking as argument the gradient vector norms of the evolving image $U(\bullet,t)$ [1]. Using the notation $U(x,y,0) = I(x,y)$, the equation corresponds to:

$$\frac{\partial U}{\partial t} = \text{div}(g(|\nabla U|)\nabla U), \quad (1)$$

with the solution of the equation for some time instant t (or observation scale) being approximated on the numerical domain by an iterative filter which computes recursively solutions from fine to coarser scales (i.e. higher t values).

A common formalism used in the literature to describe the action of a PDE-based filter is based on a moving orthonormal basis. Let $\eta = \nabla U / |\nabla U|$ denote the vector collinear with the edge direction passing through a pixel and $\xi \perp \eta$ a vector oriented along the structure direction. For each pixel, (1) can be put then in the following terms:

$$\frac{\partial U}{\partial t} = c_\xi U_{\xi\xi} + c_\eta U_{\eta\eta} \quad (2)$$

with $c_\xi = g(|\nabla U|)$ and $c_\eta = [|\nabla U|g(|\nabla U|)]'$ representing the diffusion coefficients along the two axes. Equation (2) allows a better comprehension of the filter's behavior. It can be shown that for the choice in [1]:

$$g(s) = [1 + (s/K)^2]^{-1}, \quad (3)$$

the diffusion coefficients along are always positive. Along the diffusion axis they can be positive (for $|\nabla U| < K$) or negative (for $|\nabla U| > K$), inverting in the second case the smoothing process. K represents the diffusion threshold.

Both the robustness of the process with respect to noise and its mathematical properties were addressed in several publications. We only refer here to the work of Catte et al. [2] which shows that from a practical point of view, a pre-convolution with a 2D Gaussian kernel of standard deviation σ (G_σ) improves the denoising performance of the filter for very noisy images. Equation (1) can be modified to account for this beneficial effect by a simple replacement of the diffusion function:

$$g(|\nabla U|) \rightarrow g(|G_\sigma * U|) = g(|\nabla U_\sigma|) \quad (4)$$

The aforementioned models are not addressing problems that may arise due to the influence of the noise on the determination of the diffusion directions, namely that for heavily degraded images, the diffusion directions in (2) may become false and parasite low pass filtering may occur across edges.

Several authors addressed this issue using more elaborated methods for the estimation of the diffusion directions [3], [4]. Most of these methods are based on a supplementary structure tensor-based orientation estimation step, classically known to be robust against Gaussian-like additive noise. The main idea is to set the diffusion axis to be collinear with the eigenvectors of the structure tensor: \mathbf{u} - pointing in the directions of the structures and \mathbf{v} - orthogonal to \mathbf{u} . Most corresponding filters can be written as follows:

$$\frac{\partial U}{\partial t} = c_u U_{uu} + c_v U_{vv} \quad (5)$$

with U_u , U_v and U_{uu} , U_{vv} denoting the first and, respectively, the second order directional derivatives along the \mathbf{u} and \mathbf{v} vectors. All the filters included in this class strongly limit

low-pass filtering effects in the vicinity of junctions by appropriate choices for the diffusion coefficients.

Other issues such as relationships with curve evolution, energy minimization problems or deblurring actions were addressed by numerous researchers; we refer to [5] for a complete review. 2D PDE filters were extended for the three-dimensional space; we only mention here the approaches used in [6],[7] for 3D extensions of the classical diffusion equation, in [8] for a 3D PDE-based filter that uses a diffusion tensor instead of scalar diffusivity functions and in [9] for denoising data on curved surfaces.

II. PROPOSED METHOD

For processing volume data we propose a method that employs the formalism described by (5), acting on orthogonal section planes of the 3D space. On each plane we use diffusion axes computed at a semi-local scale for increased robustness with respect to noise and we employ, on both directions, Perona-Malik like diffusivity functions (3). The filter is based on the preliminary results included in [10] and [11] and it is introduced progressively in the following sub-sections.

A. Diffusion axis

Evolved PDE-based models are all relying on a semi-local based orientation step, needed for the robust estimation of the diffusion axes. Structure tensor based approaches are presenting the advantages that they are fast, that natural extensions to any dimension are immediate and that the estimated orientation is robust with respect to white, additive Gaussian noise degradations. Nevertheless, such orientation estimation operators are only suitable for characterizing flow like patterns. On junctions and corners such approaches are always issuing false orientation information, computed as a weighted mean of the orientations of the gradient vectors falling in their support window.

An operator allowing for symmetric and asymmetric 2D image orientation estimation was proposed in [12]. Called IRON (Isotropic Recursive Oriented Network), the operator uses planar sliding windows on which a homogeneity-like measure is computed. These windows are rotated and the orientation estimation in a given pixel corresponds to the steered window showing maximal homogeneity. Moreover, the asymmetric version of the operator allows for minimizing errors nearby junctions and corners.

Based on these properties and on the results reported in [10] and [11], we employ this operator for determining the moving 2D orthonormal basis, \mathbf{u} and \mathbf{v} , that defines the directions of which the 3D filter processes each voxel, on the section planes of the processed volume.

B. Continuous model

In [10] we introduced the following PDE:

$$\frac{\partial \mathbf{U}}{\partial t} = \frac{\partial}{\partial \mathbf{u}} [g(\mathbf{U}_{\sigma_u}) \mathbf{U}_u] + \frac{\partial}{\partial \mathbf{v}} [g(\mathbf{U}_{\sigma_v}) \mathbf{U}_v]. \quad (6)$$

In its non regularized form ($\sigma=0$), (6) corresponds to a directional interpretation of an anisotropic diffusion equation acting along diffusion directions estimated in [11] at a semi-local scale, using a structure tensor-based approach.

The directional derivative along this axis (\mathbf{U}_u) acts as a confidence measure in the estimated orientation, and

depending on the relationship with a threshold parameter K_u , the filter can smooth or enhance along the structure directions. For reasonable noise levels, this occurs preferentially on junctions and the method can preserve or even enhance across scales this type of patterns. This PDE model was also used in [13] under a semi-differentiability constraint along the \mathbf{u} direction, estimated via the IRON operator. The semi-differentiability hypothesis is benefic for junctions and corners but leads to less efficient smoothing of oriented patterns. We drop this constraint in the formulation of the 3D filter.

The PDE model that we propose is based on a section plane formulation of the diffusion equation. For a 3D data volume, we first compute the maximum homogeneity direction on each section plane ($x_i O x_j$ – see *Figure.1*); let these directions be denoted by \mathbf{u}_{ij} . The second diffusion axes are then determined as being collinear to the 2D vectors orthogonal, in the considered section plane, to \mathbf{u}_{ij} ($\mathbf{u}_{ij} \perp \mathbf{v}_{ij}$).

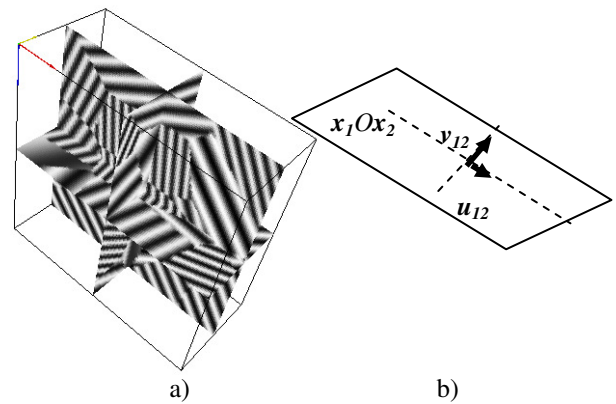


Figure. 1. Volume data. a) Section planes of a data volume. b) Diffusion axes on a section plane.

Using these notations, we formulate our PDE-based filter for volume data as below:

$$\frac{\partial \mathbf{U}}{\partial t} = \sum_{i,j} \left\{ \frac{\partial}{\partial \mathbf{u}_{ij}} [g(\mathbf{U}_{\sigma_{u_{ij}}}) \mathbf{U}_{u_{ij}}] + \frac{\partial}{\partial \mathbf{v}_{ij}} [g(\mathbf{U}_{\sigma_{v_{ij}}}) \mathbf{U}_{v_{ij}}] \right\} \quad (7)$$

The method takes as parameters the size of the support window for the IRON operator, the stopping time t and the diffusion thresholds K_u , K_v . Since IRON-based orientation estimation is being computationally extensive, we only estimate once the diffusion axes, on the initial, degraded image and we use as homogeneity criterion the variance of the gray levels. The diffusion thresholds along all the planar maximum homogeneity directions and on the orthogonal axis are set as indicated on the experimental section.

C. Numerical aspects

For the discrete filter corresponding to (7) we used forward time discretization and we approximated spatial derivatives using the classical Perona-Malik scheme on each section plane and for each diffusion axis. This translates, in a given plane $x_i O x_j$, into a forward and backward difference operators-based scheme and the needed sub-pixel resolution is handled using classic biquadratic interpolations as indicated in [10]. Similar approximations hold also for the orthogonal axis \mathbf{v}_{ij} .

III. EXPERIMENTAL EVALUATION

To evaluate the efficiency of our method we have generated synthetic data blocks composed of sinusoidal oriented patterns with different amplitudes and spatial frequencies. The experimental plan considered two categories of noise: a first category including moderate noise levels corresponding to Gaussian noise standard deviations $\sigma = 30 \div 40$ and a second category of heavier degradations corresponding to $\sigma = 50 \div 60$.

Each category included seven independent data blocks composed of $122 \times 122 \times 58$ voxels and we quantified the denoising performance by two classic measures: the classical peak signal-to-noise ratio (PSNR) and the 3D extension of structural similarity index measure (SSIM).

We used the 3D extension of the anisotropic diffusion equation (3D-AD) as a reference and we also performed comparisons with a state-of-the-art PDE-based method for denoising this type of images: the seismic fault preserving diffusion filter (SFPD [8]). We also included in our experimental plan a state-of-the-art non-PDE method: the video denoising block matching approach (VBM3D [14]), reported to produce impressive results on time-dependent, volume data. VBM3D belongs to the class of block matching approaches ([15], [16]) that employ collaborative filtering principles for finding similar data patches, grouping them onto blocks and applying shrinkage operations on the transform domain for denoising all the 2D patches within the block.

The obtained results are shown in Table 1 and the original, noisy and processed blocks are published online at the following address: http://ares.utcluj.ro/pde_denoise.html.

Visual results for both degradation categories for the best classified two filters are shown in Figures 2 and 3 for data blocks falling into each category. For easing the presentation of the results we will denote in the sequel by front, right and

top the x_2Ox_3 , x_1Ox_3 and, respectively, the x_1Ox_2 section planes of the 3D volume.

Being introduced for video denoising, the use of VBM3D for 3D data is not straightforward; one has to choose in which section planes denoising should take place i.e. which plane should be interpreted as a video-frame. We used the author's implementations [17] and we obtained the best results in denoising front section planes. These results are reported in Table 1. In each front plane, the VBM3D's results (Figure 2 b)) are close to the results obtained with our method but the filter is less efficient in eliminating noise on the right and top planes. This effect penalizes the VBM3D's performance, especially for heavily degraded blocks.

The SFPD filter uses structure tensor-based orientation estimation and an elaborated choice of the eigenvalues of the diffusion tensor, leading to adaptive unidirectional or bidirectional smoothing actions. Despite being specially designed to handle faults in seismic data, false orientations issued by orientation analysis step and the pure smoothing action of the filter can destroy high frequency content in the vicinity of junctions (Figure.2. b)) .

The proposed approach uses more reliable orientation information and, by allowing junction and edge enhancement to take place, it performs better in preserving high frequency information on these regions, having also good denoising properties on the oriented part as shown in Figure 2 c) and Figure 3 c).

We investigated the statistical relevance of the results shown in Table 1 via an analysis of variance (ANOVA) performed on the increasing rank-transformation on the SSIM values corresponding to the lower half of Table I, on the SSIM values.

Table 1 Quantitative measures on synthetic data blocks

Block label	Degraded block SSIM and PSNR		Method label							
	PSNR [dB]	SSIM	3D-AD		SFPD		VBM3D		Proposed approach	
			PSNR [dB]	SSIM	PSNR [dB]	SSIM	PSNR [dB]	SSIM	PSNR [dB]	SSIM
B1	18.59	0.9149	22.08	0.9662	26.68	0.9856	27.93	0.9893	27.93	0.9897
B2	17.50	0.8819	23.29	0.9633	26.30	0.9819	27.25	0.9859	27.32	0.9861
B3	17.24	0.8828	22.81	0.9614	26.78	0.9851	27.16	0.9863	27.36	0.9871
B4	16.75	0.8865	22.09	0.9602	26.07	0.984	26.6	0.9863	26.77	0.9867
B5	18.03	0.8894	23.60	0.9646	26.80	0.9835	27.96	0.9873	27.78	0.9869
B6	16.54	0.8597	22.43	0.955	26.39	0.9826	26.69	0.9839	26.81	0.9845
B7	16.09	0.8499	22.43	0.9574	26.11	0.9822	26.35	0.9834	26.58	0.9844
Mean	17.25	0.8803	22.68	0.9608	26.45	0.9834	27.14	0.9860	27.22	0.9864
B8	13.01	0.7321	20.89	0.9368	24.69	0.9749	24.01	0.9695	25.31	0.9782
B9	13.65	0.7805	20.74	0.9398	24.43	0.9758	24.41	0.9751	24.81	0.9776
B10	12.56	0.707	21.12	0.9361	24.74	0.9738	23.49	0.9637	25.05	0.9753
B11	13.32	0.771	20.61	0.939	24.66	0.9769	24.33	0.9749	25.10	0.9793
B12	14.15	0.6409	21.74	0.9478	25.19	0.9782	25.09	0.9776	25.75	0.9805
B13	16.76	0.6487	20.50	0.932	24.68	0.9758	24.10	0.9718	24.71	0.976
B14	13.81	0.7649	21.29	0.941	25.25	0.977	24.72	0.975	25.68	0.9794
Mean	13.90	0.7207	20.98	0.9389	24.80	0.9761	24.31	0.9725	25.20	0.9780

Table 2 Analysis of variance for the results in table 1 High noise levels

Source of variance	Sum of squares	Degrees of freedom	Mean squares	F	p
Total	1788.43	27	66.24		
Image	362.43	6	54.40		
Method	1373	3	457.67	92.56	2.9E-12
Residual	89	18	4.94		

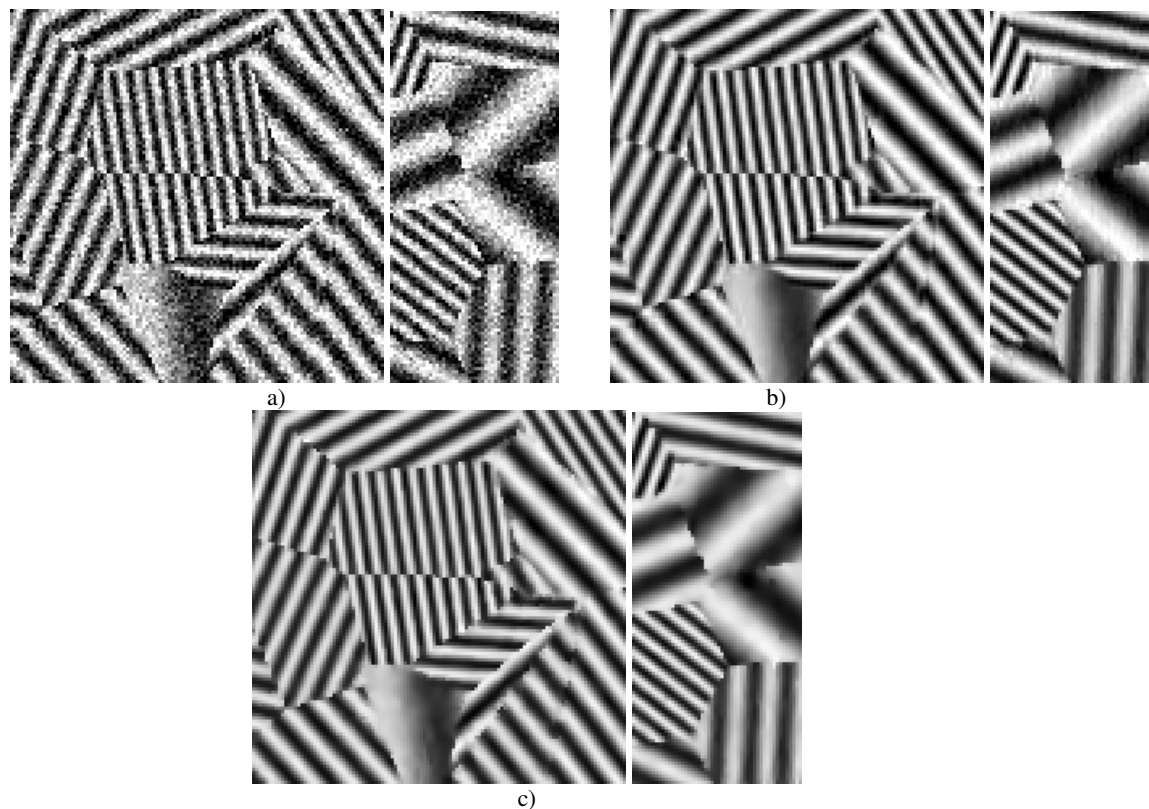


Figure. 2. Front and right slices of the synthetic data block B4. a) Noisy block; b) Result using the VBM3D approach; c) Result obtained using the proposed method.

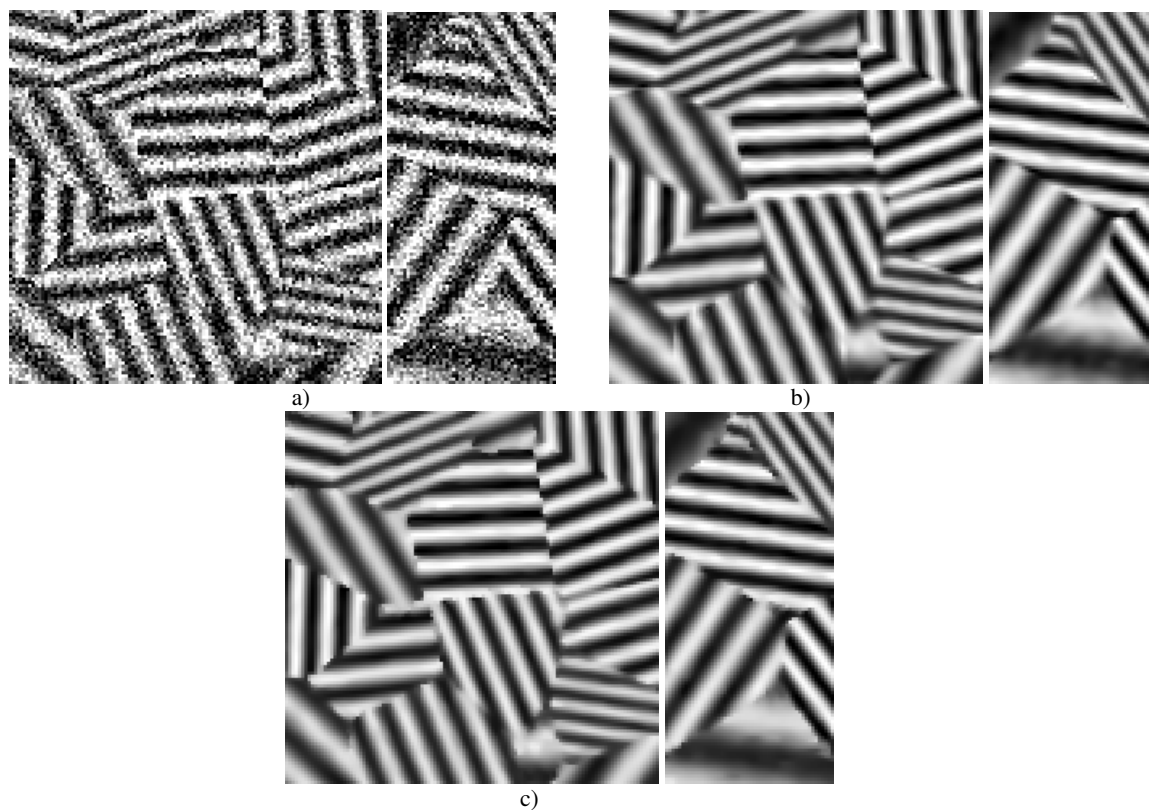


Figure.3 Front and right slices of the synthetic data block B10. a) Noisy block; b) Result using the SFPD approach; c) Result obtained using the proposed method.

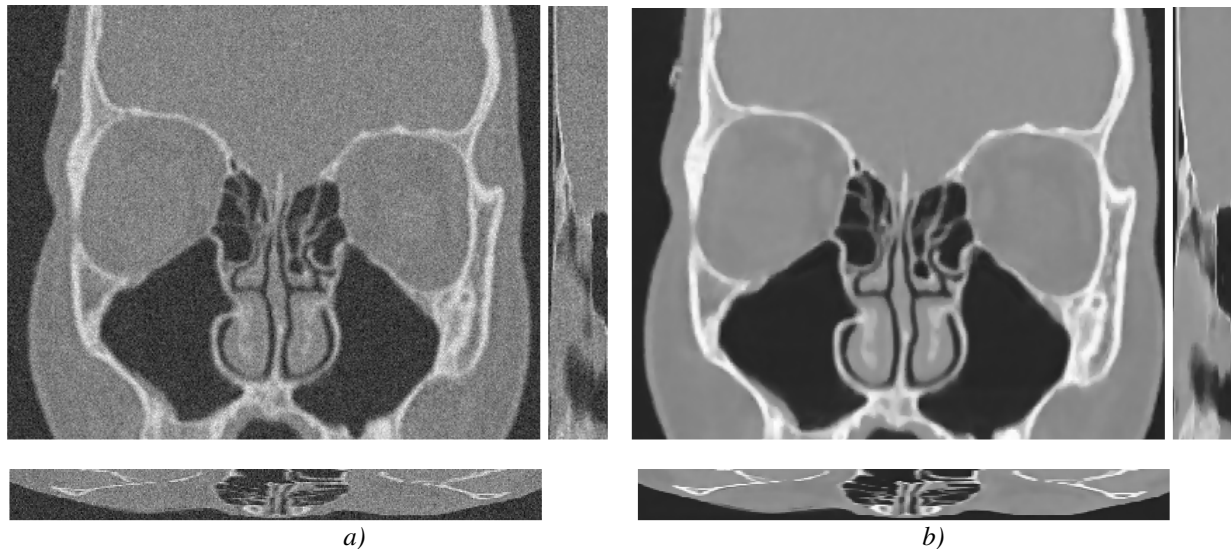


Figure.4 Front, right and top slices of a real block. a) Noisy block; b) Result obtained using the proposed method

The results are included in *Table 2* and they are showing that the choice of a specific processing method has a significant statistical influence on the quality of the obtained results.

Starting from the ANOVA analysis [18] we then used a Student-Newman-Keuls test for performing post-hoc multiple means comparisons. On high noise conditions, the proposed approach (mean rank 23.14) proved to be statistically better than the SFPD approach (rank 17.43) which, at its turn, proved to be better statistically than the VBM3D approach (rank 12.86). On the intermediate noise category the proposed approach and the VBM3D method proved to be statistically equivalent, followed, by the SFPD filter and then by 3D-AD equation.

We show in *Figure 4* results on denoising a CT scan volume data. The original scan was artificially degraded with a Gaussian noise of standard variation 25. The result shows that our approach is capable of efficiently eliminating noise, handling efficiently both oriented patterns and non-oriented regions.

Our method takes as parameters essentially seven values, the diffusion thresholds on each direction of the space and the standard deviation of the Gaussian kernel used for pre-smoothing. In all our experiments we set these values as described below. For each slice we first computed the distributions of the absolute values of the directional derivatives in the corresponding section plane, taken along the u_{ij} and, respectively, the v_{ij} diffusion axis. We then set the diffusion thresholds along these axis as being equal to a quantile (0,5) of these distributions. Such a choice induces decreasing diffusion thresholds and leads to a relative independence of the stopping time.

As far as the standard deviation of the Gaussian pre-smoothing kernel is concerned, for all our experiments we used a predefined value ($\sigma=0,75$), corresponding to a 5×5 pre-smoothing kernel.

IV. CONCLUSIONS

We propose an approach based on the partial differential equations theoretical framework for volume data denoising. This approach can efficiently eliminate Gaussian noise ensuring also efficient preservation of junctions and corners. Possible applications exist in the field of 3D material characterization or seismic imagery.

Future work will be devoted for proposing a model that can handle non-Gaussian, speckle and image dependent noise.

REFERENCES

- [1] P. Perona, and J. Malik, "Scale space and edge detection using anisotropic diffusion," *IEEE Trans. Pattern Anal. Mach. Intell.* vol. 12, no. 7, pp. 629-639, Jul., 1990.
- [2] F. Catte, P.L. Lions, J.M. Morel, and T. Coll, "Image selective smoothing and edge detection by nonlinear diffusion," *SIAM J. Numer. Anal.* vol. 29, no.1, pp.182-193, Feb. 1992.
- [3] J. Weickert, "Coherence enhancing diffusion", *Int. J. Comput. Vision*, vol. 31, no. 2, pp. 111-127 Apr., 1999.
- [4] D. Tschumperlé, and R. Deriche, "Vector-valued Image Regularization with PDE's. A common framework for different applications", *IEEE Trans. Pattern Anal. Mach. Intell.* vol. 27, no. 4, pp. 506-517, Apr., 2005.
- [5] G. Aubert, and P. Kornprobst, *Mathematical Problems in Image Processing. Partial Differential Equations and the Calculus of Variations*, New York: Springer-Verlag, 2006, ch. 3.
- [6] Q.Sun, J.A. Hossack, J. Tang, and S. Acton, "Speckle reducing anisotropic diffusion for 3D ultrasound images," *Comput. Med. Imaging Graphics*, vol.28, pp. 461-470, 2004.
- [7] Z. Hossain, T. Möller, "Edge Aware Anisotropic Diffusion for 3D Scalar Data" *IEEE Transactions on Visualization and Computer Graphics (Proceedings Visualization / Information Visualization 2010)*, vol. 16, no. 6, pp. 1375—1384, 2010.
- [8] O.Lavialle, S. Pop, C. Germain, M. Donias, S. Guillon, N. Keskes and Y. Berthomieu, "Seismic fault preserving diffusion," *J. Appl. Geophys.*, vol.61, no.2, pp.132-141, Feb., 2007.
- [9] H. Biddle, I.von Glehn, C. B. MacDonald, T. Maerz, "A volume-based method for denoising on curved surfaces", *In Proc. of the 2013 IEEE International Conference on Image Processing (ICIP 2013)*, Melbourne, 2013, pp.529-533.
- [10] R. Terebes, M. Borda, Y. Baozong, O. Lavialle, and Baylou, P., "A new PDE based approach for image restoration and enhancement using robust diffusion directions and directional

- derivatives based diffusivities," *In Proc. 7th IEEE International Conference on Signal Processing*, Beijing, 2004, pp. 707-712.
- [11] S. Pop, R. Terebes, J.P. daCosta, C. Germain, M. Borda, C. Ludusan, and O. Laviaille, "A novel 3D anisotropic diffusion filter," *In Proc. SPIE Three-Dimensional Image Processing (3DIP) and Applications*, San-Jose, 2010, vol. 7526, pp 03-13.
- [12] F. Michelet, J. P. Da Costa, O. Laviaille, Y. Berthoumieu, P. Baylou, C. Germain, "Estimating local multiple orientations," *Signal Processing*, vol. 87, no.7, pp.1655-1669, Jul.,2007
- [13] R. Terebes, O. Laviaille, C. Germain, M. Borda, and Sorin, Pop, "Asymmetric anisotropic diffusion," *In Proc. 16th IEEE International Conference on Image Processing*, Cairo, pp. 3889-3892, 2009.
- [14] K. Dabov, A. Foi, V. Katovnik, and K. Egiazarian, "Video denoising by sparse 3D transform-domain collaborative filtering," *In Proc. 15th European Signal Processing Conference*, 2007.
- [15] K. Dabov, A. Foi, V. Katovnik, and K. Egiazarian, "Image denoising by sparse 3D transform-domain collaborative filtering," *IEEE Trans. Image Process.*, vol. 16, no. 8, August 2007.
- [16] M. Maggioni, V. Katovnik, K. Egiazarian, A. Foi, "A Nonlocal Transform-Domain Filter for Volumetric Data Denoising and Reconstruction", *IEEE Trans. Image Process.*, vol. 22, no. 1, pp. 119-133, Jan. 2013
- [17] Image and video denoising by sparse 3D transform-domain collaborative filtering [Online]. Available: <http://www.cs.tut.fi/~foi/GCF-BM3D/> [Accessed: October 20, 2014].
- [18] W.J. Conover, and R.L Imam, "Rank transformations as a Bridge between Parametric and Nonparametric Statistics," *The American Statistician*, vol 35, no.3, pp. 124-129, Aug.1981.